

Interaction of Pyridine with Water in Aqueous Solution Studied by Soft X-ray Absorption Spectroscopy in C and N K-edges

M. Nagasaka, H. Yuzawa and N. Kosugi

Institute for Molecular Science, Myodaiji, Okazaki 444-8585, Japan

Pyridine is liquid and is soluble in water at any concentration. In aqueous pyridine solution, the formation of hydrogen bond (HB) between the N site of pyridine and the H site of water is proposed by the vibrational spectroscopy [1]. But the local structure of pyridine-water mixture is unknown. Soft X-ray absorption spectroscopy (XAS) is an element specific method applicable to the local structure study. In the present work, we have measured the C and N K-edge XAS of pyridine-water mixtures at different concentrations, and investigated the interaction of the C and N sites of pyridine with water in the binary solutions.

The experiments were performed at BL3U. XAS of liquid samples were measured by a transmitted-type liquid cell at room temperature [2]. The liquid layer was sandwiched between two 100 nm-thick Si_3N_4 membranes. The thickness of the liquid layer is controllable between 20 and 2000 nm by adjusting the He backpressure.

Figure 1(a) shows the C K-edge XAS of pyridine gas and pyridine-water solution $(\text{C}_5\text{H}_5\text{N})_x(\text{H}_2\text{O})_{1-x}$. The transition $\text{C } 1s \rightarrow \pi^*$ shows two peaks: First peak (C1) is derived from the meta- and para-C sites of pyridine. The second peak (C2) is the ortho-C sites. From gas to liquid pyridine ($X=1.0$), both the C1 and C2 peaks are shifted to the lower photon energy. Figure 1(b) shows the N K-edge XAS of pyridine gas and pyridine-water solutions. The $\text{N } 1s \rightarrow \pi^*$ peak shows the higher energy shift from gas to liquid. These energy shifts are consistent with those of the pyridine clusters with an antiparallel structure [3] but are smaller than in the cluster case.

By increasing the molar fraction of water in pyridine-water solution, the XAS peaks are shifted as shown in Fig. 1. Table 1 shows the peak shifts of pyridine-water mixtures from that of liquid pyridine. The C1 peaks related to the meta- and para-C sites are not changed at different concentrations. The C2 peaks related to the ortho-C sites are slightly shifted to the higher photon energy by increasing the molar fraction of water. The N peaks are more evidently shifted to the higher photon energy. The interactions of both the N and ortho-C sites with water are increased, and the interactions of the meta- and para-C sites with water are not increased because these sites are apart from water. These energy shifts are reasonable, assuming that the energy shift arises from the HB with water and the HB is formed between the N site of pyridine and water in the pyridine-water binary solutions.

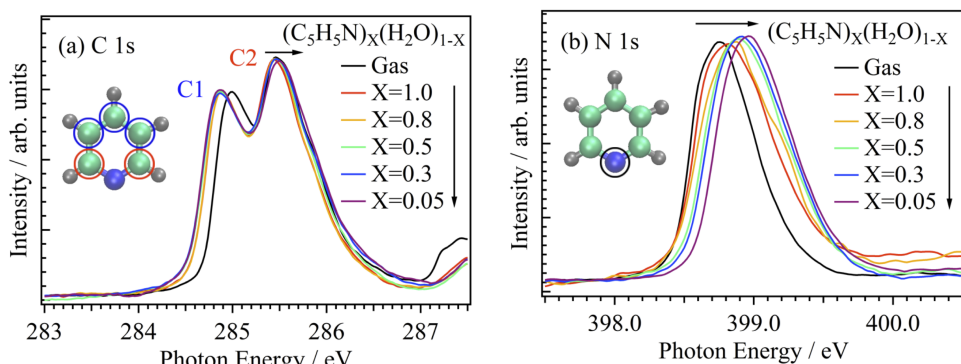


Fig. 1. XAS spectra of pyridine-water mixtures at different concentrations in (a) C and (b) N K-edges. The XAS spectra of pyridine gas are also shown. The peaks are shifted to the direction of arrows by increasing the molar fraction of water.

Table 1. Peak energy shifts (eV) of pyridine-water mixtures from liquid pyridine ($X=1.0$).

$(\text{C}_5\text{H}_5\text{N})_x(\text{H}_2\text{O})_{1-x}$	C1	C2	N
Gas	0.11	0.02	-0.07
X=1.0	-	-	-
X=0.8	0.01	0.00	0.02
X=0.5	-0.01	0.02	0.08
X=0.3	-0.01	0.02	0.08
X=0.05	-0.01	0.05	0.13

[1] S. Schlücker *et al.*, J. Phys. Chem. A **105** (2001) 9983.

[2] M. Nagasaka *et al.*, J. Electron Spectrosc. Relat. Phenom. **177** (2010) 130.

[3] I. L. Bradeanu *et al.*, J. Phys. Chem. A **112** (2008) 9192.

Interaction of Acetonitrile with Water in Aqueous Solution Studied by Soft X-ray Absorption Spectroscopy in C and N K-edges

M. Nagasaka, H. Yuzawa and N. Kosugi

Institute for Molecular Science, Myodaiji, Okazaki 444-8585, Japan

Acetonitrile is liquid and is soluble in water at any molar fraction. In aqueous acetonitrile solution, two models of the acetonitrile-water dimer were proposed [1]: One is a hydrogen bond structure between the N site of acetonitrile and the H site of water. The other is a dipole-bonded structure that water is parallel to the $C\equiv N$ group of acetonitrile by the dipole interaction. Huang et al. measured the O K-edge X-ray absorption spectra (XAS) [2] and proposed that the dipole-bonded dimer is abundant compared to the hydrogen bond structure. However, the interaction has not yet been studied from the acetonitrile side. In this study, we have measured the C and N K-edge XAS of acetonitrile-water solutions at different concentrations, and revealed the interaction of the $C\equiv N$ group of acetonitrile with water.

The experiments were performed at BL3U. XAS of liquid samples were measured by a transmitted-type liquid cell [3]. The liquid layer was sandwiched between two 100 nm-thick Si_3N_4 membranes. The thickness of the liquid layer is controllable between 20 and 2000 nm by adjusting the He backpressure.

Figure 1 shows the C and N K-edge XAS spectra of acetonitrile gas and acetonitrile-water solution $(CH_3CN)_x(H_2O)_{1-x}$. From gas to liquid acetonitrile ($X=1.0$), both the $C\ 1s \rightarrow C\equiv N\ \pi^*$ and $N\ 1s \rightarrow C\equiv N\ \pi^*$ peaks are shifted to the higher photon energy. It is because liquid acetonitrile shows the antiparallel structure between the $C\equiv N$ groups of acetonitrile by the dipole interaction.

Table 1 shows the peak shifts of acetonitrile-water mixtures from that of liquid acetonitrile. The C peak is shifted to the higher energy by increasing the molar fraction of water. On the other hand, the N peak is shifted to the lower energy. The interaction of the C site of the $C\equiv N$ group is increased by water, and that of the N site is slightly decreased. These results suggest that the acetonitrile-water solution may have the dipole-bonded structure, in which the oxygen site of water is close to the C site of the $C\equiv N$ group of acetonitrile. It should be also noted that the peak width at $X=0.05$ is narrower than those at different molar fractions, suggesting that in dilute aqueous solutions acetonitrile may be isolated by the dipole interaction with water.

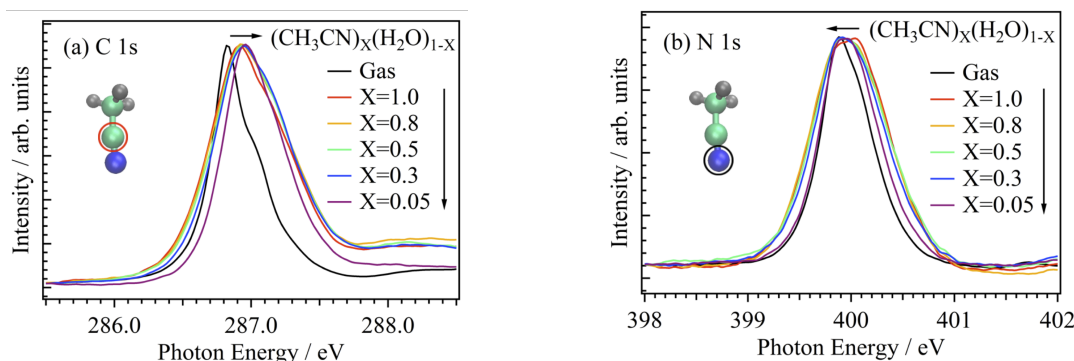


Fig. 1. XAS spectra of acetonitrile-water mixtures at different concentrations in (a) C and (b) N K-edges. The XAS spectra of acetonitrile gas are also shown. The peaks are shifted to the direction of arrows by increasing the molar fraction of water.

Table 1. Peak shifts of acetonitrile-water mixtures from that of liquid acetonitrile ($X=1.0$).

$(CH_3CN)_x(H_2O)_{1-x}$	C	N
Gas	-0.09	-0.09
$X=1.0$	-	-
$X=0.8$	0.02	-0.02
$X=0.5$	0.02	-0.02
$X=0.3$	0.02	-0.03
$X=0.05$	0.05	-0.03

[1] I. Bakó, T. Megyes and G. Pálinkás, Chem. Phys. **316** (2005) 235.

[2] N. Huang et al., J. Chem. Phys. **135** (2011) 164509.

[3] M. Nagasaka *et al.*, J. Electron Spectrosc. Relat. Phenom. **177** (2010) 130.

Soft X-ray Absorption Spectroscopic Study of Solid-Liquid Interface

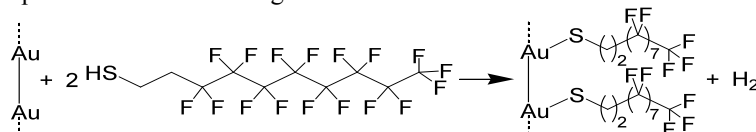
H. Yuzawa, M. Nagasaka, N. Kosugi

Institute for Molecular Science, Okazaki 444-8585, Japan

Detailed understanding of the interface interaction is important to clarify physical and chemical phenomena such as molecular adsorptions, catalytic reactions and so on. However, the solid/liquid interface is difficult to measure because it involves two different condensed phases. We generally use particle (electron, ion etc.) or light (IR, X-ray etc.) probe to investigate geometric and electronic structures, but the former interacts too strong with both phases to observe the interface. The latter only gives average information of the interface and bulk, where the information of the interface (minor component) get covered up by that of the bulk [1]. Thus, new approaches are required to measure the solid/liquid interface.

We developed a transmission-type liquid XAS (X-ray Absorption Spectroscopy) cell with Si_3N_4 or SiC windows, which is able to control easily the thickness of the liquid thin layer (20-2000 nm), for the soft X-rays [2]. From the other point of view, this liquid cell contains solid/liquid interfaces and can strengthen the information of the interface for light probe by controlling the liquid thickness. Thus, we tried to detect the interaction of solid/liquid interface in the liquid XAS cell, whose surface is modified to objective structures.

The experiments were carried out in BL3U. Two Au (thickness: 20 nm) and Cr (5 nm) deposited Si_3N_4 (100 nm) membranes were used as liquid cell windows. The model surface in this study was prepared by the modification (chemisorption) of 1H, 1H, 2H, 2H -perfluorodecanethiol (F-thiol) monolayer on the gold surface (Scheme 1). Then, the cell was filled with liquid (water or benzene) and C K-edge XAS was measured at room temperature as shown in Fig. 1.



Scheme 1. Modification of gold surface by F-thiol monolayer.

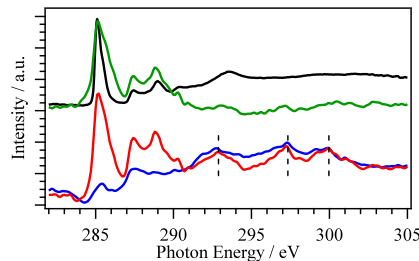
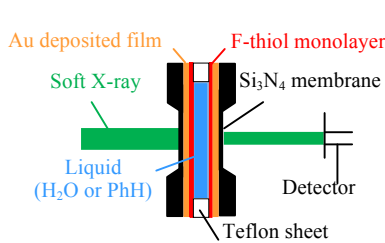


Fig. 1. Schematic (side view) of soft X-ray XAS measurement to detect the interaction at the solid/liquid interface.

Fig. 1. Schematic (side view) of soft X-ray AXS measurement to detect the interaction at the solid/liquid interface.
 Fig. 2. C K-edge XAS spectra of the modified liquid cell filled with water (blue line) or benzene (red line) and that of the unmodified one filled with benzene (black line). Green line corresponds to the spectrum of the red line subtracted by that of the blue line to remove the influence of the absorption of F-thiol.

Figure 2 shows the C K-edge XAS spectra of the modified liquid cell filled with water (blue line) or benzene (red line). In both cases, three absorption peaks (> 290 eV), which correspond to the excitation from C 1s to σ^* of F-thiol, were observed. It was confirmed that this system could detect the soft X-ray absorption of molecule at the solid/liquid interface. Nevertheless, the energy positions of each absorption peak were consistent regardless of liquid phase.

On the other hand, when the absorption peak (285.1 eV, $1s \rightarrow \pi^*$) of benzene (green line) extracted from the red line was compared with that without the liquid cell modification of F-thiol (black line), the width of the absorption peak broadened. This would be because the electronic state of benzene molecule was influenced by the interactions between the F atom in F-thiol and the benzene molecule at the interface, e.g., $-F \cdots H-$ interaction [3] and $-F \cdots \pi$ interaction [4]. Thus, the trace of the interface interaction could be detected in the liquid side

Through the above experiments, we can conclude that the transmission soft X-ray XAS approach has a potential to detect the interaction of solid/liquid interface.

- [1] F. Zaera, Chem. Rev. **112** (2012) 2920.
 - [2] M. Nagasaka *et al.*, J. Electron Spectrosc. Relat. Phenom. **177** (2010) 130.
 - [3] M.D. Prasanna *et al.*, Cryst. Eng. **3** (2000) 135.
 - [4] B. Brammer *et al.*, New J. Chem. **23** (1999) 965.

In-situ Observation of Electrochemical Reaction by Soft X-ray Absorption Spectroscopy with Potential Modulation Method

M. Nagasaka, H. Yuzawa, T. Horigome and N. Kosugi
Institute for Molecular Science, Myodaiji, Okazaki 444-8585, Japan

For understanding the electrochemical reaction, it is most important to investigate local structures of electrolytes including electric double layers at different potentials. Soft X-ray absorption spectroscopy (XAS) is an element specific method to study local electronic structures of solutions and interfaces. Recently, we developed a liquid cell for XAS in transmission mode [1], in which the thickness of the liquid layer is controllable between 20 and 2000 nm. In addition, we successfully measured XAS of electrolytes in electrochemical reaction by using a liquid cell with built-in electrodes [2]. From the Fe L-edge XAS spectra of aqueous iron sulfate solutions in electrochemical reaction, we revealed change in the valence of Fe ions at different potentials, where each XAS spectrum was measured at a constant potential and the scanning rate of the potential (0.08 mV/s) was quite slower than that in regular cyclic voltammetry (CV) (typically 100 mV/s). In this study, we have developed a potential modulation method to make possible in-situ XAS observation of electrochemical reaction at the same scanning rate of CV.

In the XAS measurement with a potential modulation method, the electrode potential is swept at a fixed photon energy, and soft X-ray absorption coefficients at different potentials are measured at the same time. After repeating the potential modulation at different photon energies, we can get XAS of electrolytes in electrochemical reaction at the same scanning rate of CV.

The experiments were performed at BL3U. XAS spectra of electrolytes were measured by using a liquid cell with built-in electrodes [2]. Figure 1 shows the Fe L-edge XAS spectra of aqueous iron sulfate solutions in electrochemical reaction at 100 mV/s. By increasing the potential from 0.0 to 1.0 V, the peak intensity of Fe(II) (708 eV) is decreased and that of Fe(III) (710 eV) is increased by the oxidation of Fe(II). By decreasing the potential from 1.0 to -0.4 V, the peak intensity of Fe(II) is increased, and that of Fe(III) is instead decreased by the reduction of Fe(III).

To obtain the fraction of Fe(II) and Fe(III) ions, the Fe L-edge XAS spectra at different potentials are fitted by superposition of the reference XAS spectra of Fe(II) and Fe(III) ions. Figure 2 shows fractions of Fe(II) and Fe(III) ions in electrochemical reaction at 100 mV/s. By increasing the potential, the fraction of Fe(III) is increased and that of Fe(II) is decreased. The Fe(II) ions are partially changed to the Fe(III) ions by the oxidation process. It is because a thick liquid layer is necessary for XAS of dilute Fe ions in transmission mode. As shown in the inset of Fig. 2, the XAS spectra includes both the solid-liquid interface that occurs the Fe redox reaction and the bulk electrolyte of Fe(II) that does not involve the electrochemical reaction. The mechanism of these Fe redox process will be discussed by correlating the XAS results with those at the different scanning rates.

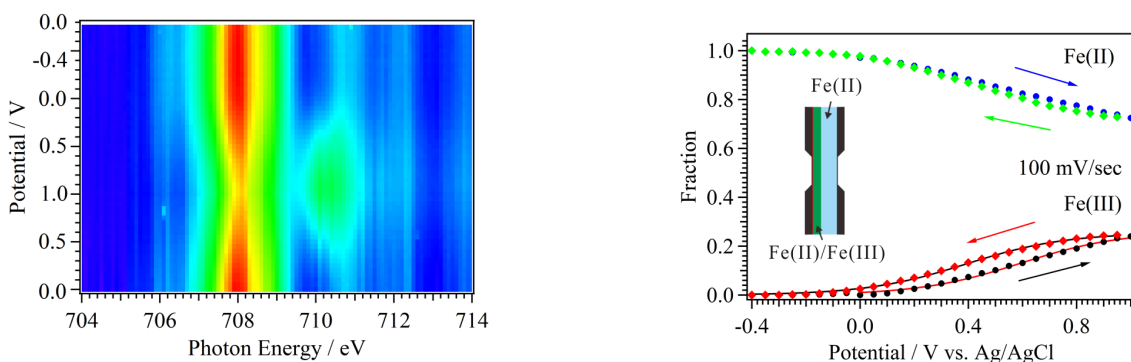


Fig. 1. Two dimensional plots, photon energy and potential (versus Ag/AgCl), of the Fe L-edge XAS spectra in electrochemical reaction of aqueous iron sulfate solutions at the scanning rate of 100 mV/s.

Fig. 2. Fractions of Fe(II) and Fe(III) ions as a function of potential (versus Ag/AgCl) in electrochemical reaction at 100 mV/s. The inset shows a partial oxidation model in a liquid cell.

[1] M. Nagasaka *et al.*, J. Electron Spectrosc. Relat. Phenom. **177** (2010) 130.

[2] M. Nagasaka *et al.*, J. Phys. Chem. C **117** (2013) 16343.

In Situ Observation of Nickel-Borate Catalyst for Oxygen Evolution Reaction by Soft X-ray Electrochemical XAFS

M. Yoshida^{1,*}, M. Nagasaka², T. Iida¹, T. Mineo¹, T. Yomogida¹, H. Yuzawa², N. Kosugi² and H. Kondoh¹

¹Department of Chemistry, Keio University, Yokohama 223-8522, Japan

²Department of Photo-Molecular Science, Institute for Molecular Science, Okazaki 444-8585, Japan

Electrochemical hydrogen production from water has attracted considerable attention due to the potential toward highly efficient energy conversion. This reaction consists of two half reactions of hydrogen and oxygen evolution. However, the efficiency of oxygen evolution reaction (OER) is insufficient for many electrode materials because of the high overpotentials. Recently, Bediako *et al.* reported that a nickel-borate thin film can function as an efficient electrocatalyst for OER and the activity was likely to be dependent on the concentration of potassium borate (KB_i) in electrolyte aqueous solution [1]. Therefore, in this study, the nickel-borate thin film was investigated by *in situ* O K-edge XAFS measurements under potential control conditions with changing the electrolyte aqueous solution.

The soft X-ray electrochemical XAFS measurements were performed with the transmission mode at BL3U of UVSOR, according to the previous works [2]. Au/Cr/SiC thin film substrates were used as working electrodes. A home-made electrochemical cell was used with a Pt mesh counter electrode and a Ag/AgCl (saturated KCl) reference electrode.

O K-edge XAFS spectra were taken for the electrodeposition reaction of nickel-borate thin film at 1.0 V vs. Ag/AgCl in a 0.1 M KB_i aqueous solution containing 0.4 mM $\text{Ni}(\text{NO}_3)_2$, as shown in Figure 1. A peak associated with oxygen species was observed at ca. 528.5 eV and kept to grow for 90 min. Next, the electrolyte solution was changed to 0.5 M KB_i aqueous solution without nickel ions and the XAFS measurements were tested with changing the applied electrode potential (Figure 2). The peak at ca. 528.5 eV disappeared at lower potential (0.5 V) and regenerated at higher potential (1.0 V) accompanying with the OER activity. In previous works of Ni K-edge XAFS [1], it is indicated that the nickel borate electrocatalyst forms μ -oxo/hydroxo nickel centers organized into higher-order domains of edge sharing NiO_6 octahedra at higher potential. Thus, our present study demonstrated the presence of the NiO_6 octahedra domain by the direct observation of oxygen species in the nickel borate thin film. When the concentration of KB_i in electrolyte solution decreased, the XAFS peak was not observed even at 1.0 V accompanying with the decrease of the OER activity, which indicates that the formation of the NiO_6 octahedra domain was suppressed. Therefore, we found that the high activity of nickel borate thin film for OER is derived from the formation of the NiO_6 octahedra domain and related with the KB_i concentration in the electrolyte aqueous solution.

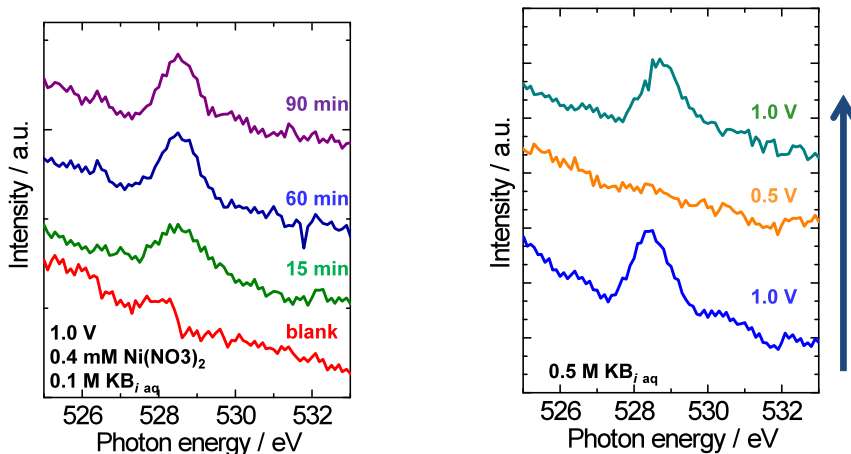


Figure 1. Time course of *in situ* O K-edge XAFS during electrodeposition reaction of nickel-borate thin film.

Figure 2. *In situ* O K-edge XAFS spectra under electrochemical control in 0.5 M KB_i aqueous solution.

[1] D. K. Bediako *et al.*, J. Am. Chem. Soc. **134** (2012) 6801., **135** (2013) 3662.

[2] M. Nagasaka *et al.*, J. Electron. Spectrosc. Relat. Phenom. **177** (2010) 130., J. Phys. Chem. C **117** (2013) 16343.

Polarized NEXAFS Study on Structure of Nitrogen Doped Rutile TiO₂(110)

Y. Monya¹, M. Yoshida¹, M. Nagasaka², H. Yamane², N. Kosugi² and H. Kondoh¹

¹Graduate School of Science and Technology, Keio University, Yokohama 223-8522, Japan

²Institute for Molecular Science, Okazaki 444-8585, Japan

Nitrogen doped TiO₂, which is one of most promising visible-light-response photocatalysts, has been extensively studied to understand the mechanism of its visible-light-response. Although many structural studies on nitrogen dopants in TiO₂ have been conducted with various techniques, neither doping site nor chemical state of the nitrogen dopant is known in detail. In this work, we measured polarized NEXAFS spectra for nitrogen doped rutile TiO₂(110) to elucidate its structure.

The samples were prepared by heating rutile TiO₂(110) substrates under NH₃ atmosphere at 1.0 Torr. Polarized NEXAFS measurements were performed at BL3U with using the partial electron yield method. The photon energies were calibrated by the energy of the first peak (530.6 eV) at O-K edge.

Fig. 1 shows O-K edge NEXAFS spectra of rutile TiO₂(110) with different polarization directions. For example, NI [001] indicates that x-ray incidence angle is 90° from the surface parallel and its electric vector is lying along the [001] direction (see Fig. 2). In the grazing incidence (GI) geometry, the incidence angle was 30°. For the O-K edge spectra, we observe five peaks (*a-e*) and they are seen in the typical spectra of rutile TiO₂(110). Considering the previous assignments for these peaks [1,2], peaks *a* and *b* can be attributed to excitations to unoccupied states: (Ti 3d + O 2p π) and (Ti 3d + O 2p σ), respectively. Peaks *c-e* are assigned to (Ti 4sp + O 2p). In NI[001] spectrum, peak *b* exhibits different polarization dependence from the other peaks. It might be because part of peak *b* is associated with a surface oxygen species shown in Fig. 2. Considering its bonding direction, the excitation to an unoccupied state of (Ti 3d + O 2p σ) character should be observed only in the [001] direction and particularly strong in NI[001]. Therefore, it can be said that the N doped rutile TiO₂(110) has a similar structure to pristine TiO₂ and the surface oxygen species bridging two Ti atoms remain after doping reactions. Fig. 3 shows N-K edge NEXAFS spectra of the nitrogen dopants in the rutile TiO₂(110), where the incidence angle was 15° for GI and 90° for NI from the surface parallel. As a result, seven peaks (*a'-d'* and X, Y, Z) were observed. Peak *a'* and *b'* can be attributed to excitations to unoccupied states: (Ti 3d + N 2p π) and (Ti 3d + N 2p σ), respectively. Peaks *c'* and *d'* are assigned to (Ti 4sp + N 2p). From these results, the doped N species are likely to occupy the lattice oxygen sites via substitution. It should be noted that peaks X, Y, Z appear exclusively in the N-K edge spectra. Based on the results of XPS, DFT calculations and a previous report [3], it is proposed that the nitrogen dopants are not only in the form of N but also in the form of NH. Thus, peaks X and Y can be attributed to excitations to NH-derived unoccupied states. Peak Z could be associated with an edge structure.

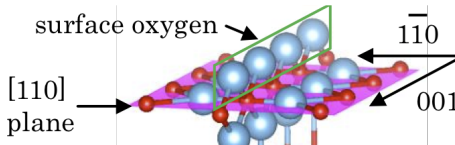


Fig. 2. Structure model for rutile TiO₂(110) surface.

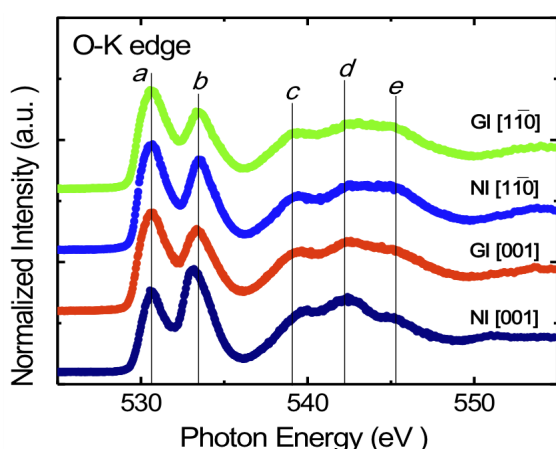


Fig. 1. O-K NEXAFS spectra of N doped rutile TiO₂(110).

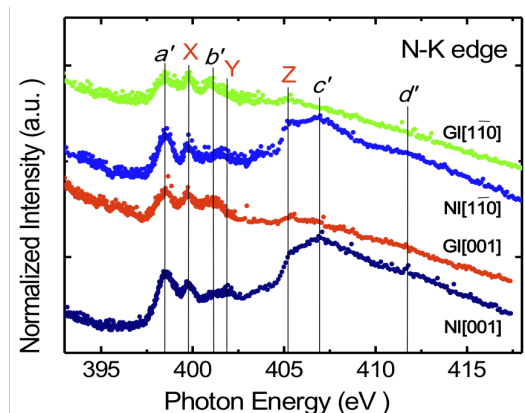


Fig. 3. N-K NEXAFS spectra of nitrogen dopants in rutile TiO₂(110).

[1] J. G. Chen, Surf. Sci. Rep. **30** (1997) 1.

[2] E. Filatova *et al.*, Phys. Status Solidi B **246** (2009) No.7, 1454.

[3] Y. Kim *et al.*, J. Phys. Chem. C **115** (2011) 18618.

Uptake of Dexamethasone into Human Skin Investigated by Soft X-Ray Spectromicroscopy

R. Flesch¹, T. Ohigashi², S. Küchler³, K. Yamamoto¹, S. Ahlberg⁴, F. Rancan⁴, A. Vogt⁴, U. Blume-Peytavi⁴, P. Schrade⁵, S. Bachmann⁵, M. Schäfer-Korting³, N. Kosugi², and E. Rühl¹

¹Physical Chemistry, Freie Universität Berlin, Takustr. 3, 14195 Berlin, Germany

²UVSOR Facility, Institute for Molecular Science, Okazaki 444-8585, Japan

³Institut für Pharmazie, Freie Universität Berlin, 14195 Berlin, Germany

⁴Charité Universitätsmedizin, 10117 Berlin, Germany

⁵Abteilung für Elektronenmikroskopie at CVK, 13353 Berlin, Germany

The uptake of drugs, such as dexamethasone, topically applied onto human skin is investigated by soft X-ray spectromicroscopy. Dexamethasone is a widely used for the treatment of inflammatory skin diseases such as atopic dermatitis. It is aimed to study the depth profile of dexamethasone, so that specific information on the uptake process is derived. Dexamethasone was dissolved in ethanol and this 0.5% solution was applied onto the skin sample for 4 h. Subsequently, the sample was fixed and sliced into 300 nm thick sections.

The experiments were performed at the BL4U beamline at UVSOR III using a scanning X-ray microscope (STXM) [1]. Chemical selectivity is obtained from excitation at the O 1s-edge (525–560 eV). Figure 1 shows a comparison of the O 1s-absorption of fixed human skin and dexamethasone. Both spectra are similar in shape, showing an intense O 1s→π* resonance dominating the pre-edge regime. This resonance occurs at slightly lower energy in dexamethasone (E=530.5 eV) than in skin (E=532.2 eV), providing chemical selectivity for probing the drug uptake into skin.

Figure 2 shows a comparison of a skin sample exposed to dexamethasone probed by optical microscopy and soft X-ray microscopy. Figure 2(a) clearly shows the layered structure of the stratum corneum, the outermost skin layer, probed by optical microscopy. It is followed by the viable epidermis and the dermis. Figure 2(b) shows for the same section of the skin sample the spatial distribution of absorption, which is obtained from a difference image in X-ray absorption measured at 528 eV (pre-edge regime) and on the O 1s→π*-transition (530.5 eV) of dexamethasone (cf. Fig. 1) providing chemical selectivity. The spatially resolved results indicate that highest absorption contrast is found in the stratum corneum, as indicated by red color. In contrast, lower concentration is observed in the viable epidermis and no change in absorption contrast occurs in the dermis. It is also evident that the cells nuclei in the viable epidermis (circular structures in Fig. 2(a)) do not show any evidence for drug uptake.

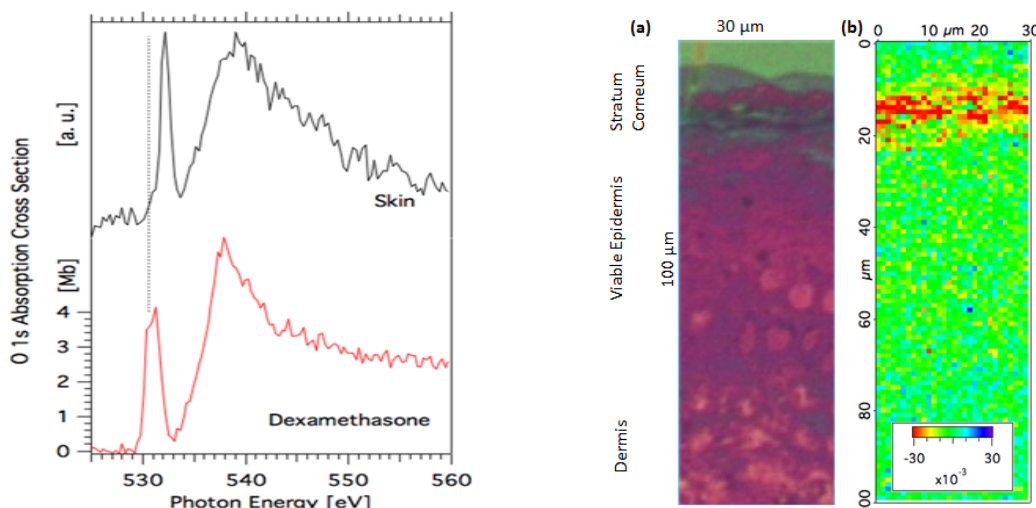


Fig. 1. O 1s excitation of fixed human skin (black curve) and dexamethasone (red curve).

Fig. 2. (a) optical microscopy image of human skin; (b) spatial distribution of dexamethasone in the same skin section, as shown in (a). See text for further details.

Observation of DNA and Protein Distributions in Mammalian Cell Nuclei using STXM

T. Ohigashi^{1,2}, A. Ito^{1,3}, K. Shinohara^{3,4}, S. Tone⁵, M. Kado⁴, Y. Inagaki¹, Y. F. Wang¹, and N. Kosugi^{1,2}

¹UVSOR Facility, Institute for Molecular Science, Okazaki 444-8585, Japan

²The Graduate University for Advanced Studies (SOKENDAI), Okazaki 444-8585, Japan

³Tokai University, Hiratsuka, Kanagawa, 259-1292, Japan

⁴Japan Atomic Energy Agency, Kizugawa, Kyoto, 619-0215, Japan

⁵Kawasaki Medical School, Kurashiki, Okayama 701-0192, Japan

To observe the structure of biological samples, an electron microscope and a fluorescence microscope are extensively used. However, the former requires specimen in vacuum and the latter has relatively lower spatial resolution. Moreover, the electron microscope usually requires several preparation processes for the samples, such as fixing, slicing and staining. On the other hand, a soft X-ray microscopy is applicable to relatively thick specimen even under hydrated condition at high resolution, and is expected to be complementary to these two types of microscopes. A scanning transmission X-ray microscope (STXM) must be a powerful tool for this purpose [1]. The STXM has high spatial resolution, high transmittance and lower radiation damage than the electron beam. Especially, chemical analysis combined with near edge X-ray absorption fine structure (NEXAFS) enables us to obtain 2-dimensional chemical information of the sample [2]. In this study, nuclei of cultured human cells were observed with the STXM installed on UVSOR BL4U to image the distributions of DNA and protein separately.

NEXAFS spectra of the DNA and histone, a nuclear protein, were measured by the STXM as reference data. Their suspensions were dropped onto 100 nm-thick silicon nitride membranes and were dried in the air. Their NEXAFS spectra around nitrogen 1s are shown in Fig. 1. In these spectra, a remarkable feature to discriminate the DNA from the protein is seen on a peak at 400.8 eV as nitrogen 1s→π* resonance arising from C=N double bonds in the DNA.

Human A549 cells derived from lung cancer were cultured directly on the silicon nitride membrane, fixed with glutaraldehyde, and dried in the air. The sample was placed in the STXM chamber, which was then evacuated and was filled by helium to 30 mbar. The 51 X-ray transmission images (an energy stack) were acquired with changing the X-ray energies from 399 to 404 eV. The dwell time and the scanning pitch of the specimen were 5 ms and 0.2 μm step, respectively. The reference spectra of the DNA and the histone in Fig. 1 were fitted to the energy stack by using aXis2000 software [3] and their distributions are shown in Fig. 2. Figures 2 (a) and (b) show distributions of the DNA and the histone (protein), respectively. Fig. 2 (c) shows the distribution of constant profile with no spectral feature, suggesting that in the nucleolus molecules other than the DNA and/or the histone (protein) are densely accumulated. The results show that the DNA was distributed over the nucleus, while the histone was poorly distributed in the nucleolus. Considering that RNA is rich in the nucleolus, the RNA may be present with less protein in the nucleolus.

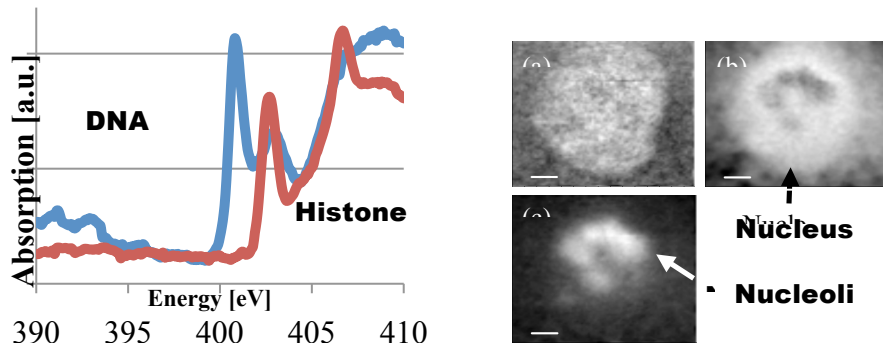


Fig. 1 X-ray absorption spectra of the DNA and the histone (protein) around nitrogen 1s resonance.

Fig. 2 Distributions of the DNA (a), the histone (protein) (b) and constant (c) in the cell.

Bright color corresponds to high density. Scale bars are 2 μm.

[1] J. Kirz *et al.*, Nucl. Instr. and Meth. B **87** (1994) 92-27.

[2] T. Ohigashi *et al.*, J. Phys. Conf. Ser. **463** (2013) 012006.

[3] <http://unicorn.mcmaster.ca/aXis2000.html>

Observation of the origin of d^0 magnetism in ZnO nanostructures using X-ray-based microscopic and spectroscopic techniques

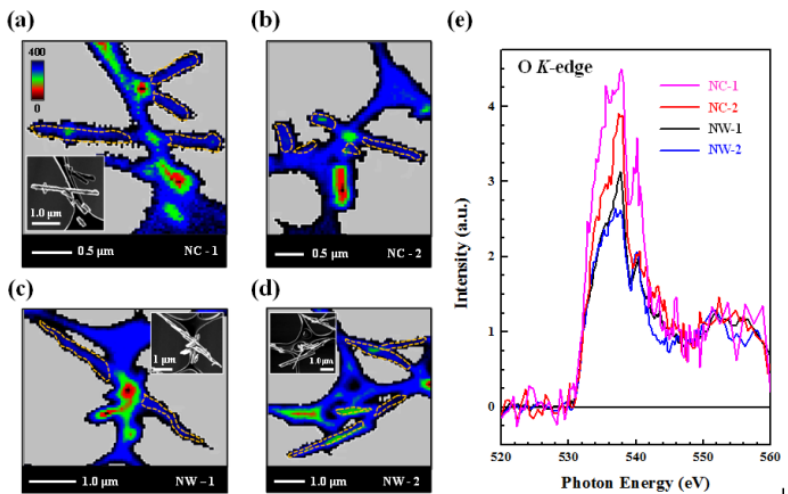
S. B. Singh¹, Y. F. Wang¹, J. W. Chiou², W. F. Pong¹, T. Ohigashi³ and N. Kosugi³

¹Department of Physics, Tamkang University, Tamsui 251, Taiwan

²Department of Applied Physics, National University of Kaohsiung, Kaohsiung 811, Taiwan

³Editorial Board, UVSOR Facility, Institute for Molecular Science, Okazaki 444-8585, Japan

In present report, efforts have been made to elucidate the origin of d^0 magnetism^{1,2} in ZnO nanocactus (NC) and nanowires (NW) using X-ray-based microscopic and spectroscopic techniques. The magnetic hysteresis curve obtained in an applied field revealed that the saturation magnetization in ZnO NC exceeded that of the NW. Fig. 1 shows the O K-edge scanning transmission X-ray microscopy (STXM) and corresponding x-ray absorption near-edge structure (XANES) spectra of the ZnO nanostructures. The experiments were performed at the 4U beamline. The O K-edge STXM stack mappings were recorded at two randomly selected regions in ZnO NC (NC-1 and NC-2) and NW (NW-1 and NW-2) respectively (see Figs. 1a-d). The insets in the figures also present corresponding scanning electron microscopy images that help to identify the regions and can be used to verify the STXM images. To overcome the signal-to-noise ratio of the XANES spectra obtained from specific mapping areas in the STXM images, the O K-edge STXM-XANES spectra in Fig. 1(e) were obtained as the sum of the XANES spectra in the regions that are bordered by yellow dashed lines, as shown in NC-1, NC-2, NW-1 and NW-2. According to the dipole-transition selection rule, the features at \sim 535–550 eV are attributed to the electron excitations from O 1s-derived states to $2p_{x,y}$ -derived (along the bilayer) and O 2p_z-derived (along the *c* axis) states, which are approximately proportional to the density of the unoccupied O 2p-derived states.³ The intensities of the O K-edge STXM-XANES spectra of NC-1 and NC-2 are clearly higher than those of NW-1 and NW-2. The STXM-XANES results consistently demonstrate that the population of defects at the O sites in ZnO NC is larger than in the NW and confirming the enhanced density of states of O 2p-derived states, as the population of defects and dangling bonds at/above E_{CBM} or E_F in ZnO NC exceeds that in the NW. The experimental results are also consistent with the measurements of extended X-ray absorption fine structure spectroscopy, X-ray excited optical luminescence spectroscopy and X-ray magnetic circular dichroism. The STXM-XANES results strongly support the arguments that the origin of magnetization is attributable to the O 2p orbitals rather than the Zn 3d orbitals.



Figs. 1 (a)-(d) O K-edge STXM images of two selected regions in ZnO NC (NC-1 and NC-2) and NW (NW-1 and NW-2), respectively. **(e)** corresponding O K-edge XANES spectra of regions bordered by yellow dashed lines in ZnO NC (NC-1 and NC-2) and ZnO NW (NW-1 and NW-2). The insets show the corresponding SEM images.

References

- [1] T. A. Dietl *et al.*, Nat. Mater. 9 (2010) 965.
- [2] S. Z. Deng *et al.*, ACS Nano 4 (2010) 495.
- [3] J. W. Chiou *et al.*, Appl. Phys. Lett. 85 (2004) 3220.

Substituent-Induced Intermolecular Interaction in Organic Crystals Revealed by Precise Band-Dispersion Measurements

H. Yamane and N. Kosugi

Department of Photo-Molecular Science, Institute for Molecular Science, Okazaki 444-8585, Japan

Solid-state functionalities of organic molecules are governed not only by individual molecular properties but also by their intermolecular interactions. This concerted interplay dominates a key process of the electric conduction in functional molecular systems. In this work, we have investigated the intermolecular energy-vs-momentum $E(\mathbf{k})$ relation, originating from the molecular stacking periodicity, of sub-100-meV scale in metal phthalocyanine (MPc) crystalline films. The small $E(\mathbf{k})$ relation of MPc with different terminal groups and central metals are sensitive and essential to characterize the intermolecular interaction in terms of the intermolecular distance, the molecular conformation, and the orbital symmetry.

Figure 1 shows the emission angle (θ) dependence of the angle-resolved photoemission (ARPES) spectra and its intensity map for the flat-lying monolayer and crystalline films of ZnPc on Au(111) at 15 K. For the monolayer, the dispersive and non-dispersive peaks appear around the binding energy (E_b) of 0~0.32 eV and 0.74 eV, respectively. The parabolic dispersion at $E_b = 0\text{--}0.32$ eV is derived from the Shockley state (SS) of the Au(111) surface, which is modified by the complex interplay of molecule-substrate interactions. The non-dispersive peak at $E_b = 0.74$ eV is derived from the highest occupied molecular orbital (HOMO) of C 2p (π) character in ZnPc. The observed HOMO- peak intensity shows a sharp θ dependence with the maximum at $\theta = 34^\circ$. This is due to the reflection of the spatial electron distribution of HOMO. For the ZnPc crystalline film, the SS band of Au(111) is suppressed and the HOMO peak is stabilized as $E_b \sim 1.3$ eV. Since the ZnPc molecule deposited on Au(111) shows the Stranski-Krastanov growth, the quite weak substrate signal of E_F appears and is utilized for the energy calibration for the precise $E(\mathbf{k})$ measurement. The θ dependence of the HOMO-peak intensity in the ZnPc crystalline film is almost the same as that in the ZnPc monolayer film; that is, the molecular orientation indicates the layer-by-layer growth in the crystalline domain and induces orbital delocalization. Indeed, the HOMO peak of the ZnPc crystalline film shows a small dispersive behavior with θ . Such a dispersive behavior is not observed in the monolayer film and is related to the delocalized band formation.

In order to investigate the \mathbf{k} component along the $\pi\text{-}\pi$ stacking direction (\mathbf{k}_\perp), we measured the normal emission ARPES as a function of the photon energy ($h\nu$) for crystalline films of various MPc (H₂Pc, MnPc, CoPc, ZnPc, and F₁₆ZnPc) on Au(111) at 15 K. From this systematic experiment, we revealed quite small but different $E(\mathbf{k}_\perp)$ relations. The transfer integral (t_\perp) of the C 2p band is found to be dependent on the intermolecular distance (a_\perp) with the 75 ± 5 meV/Å relation (see, Fig. 2). Furthermore, we observed the different dispersion phase and periodicity, depending on the terminal group and central metal in MPc, which originate from the site-specific intermolecular interaction induced by substituents [1].

As described above, precise and systematic $E(\mathbf{k})$ studies provide deeper insights into the nature of the intermolecular interaction, which further represents the importance of the site specificity in the inter-molecular interaction as a possible origin of unique molecular electronic properties.

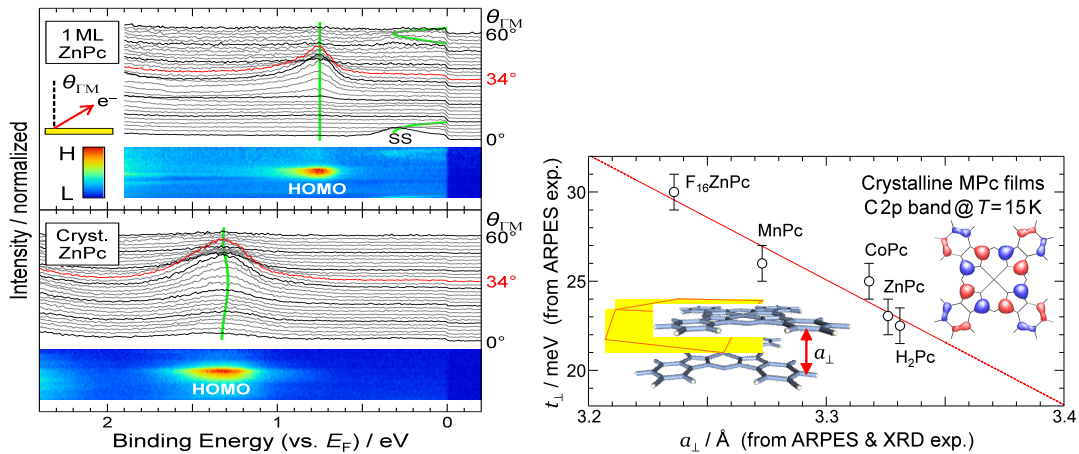


Fig. 1. The θ dependence of the ARPES spectra ($h\nu = 45$ eV) and its intensity map for the monolayer and crystalline films of ZnPc on Au(111) at 15 K.

Fig. 2. The t_\perp -vs- a_\perp relation for the C 2p band in MPc crystals at 15 K, with $t_\perp/a_\perp = 75$ meV/Å line.

Observation of Interface State and Intermolecular Band Dispersion in a Monolayer Superstructure of Coronene Physisorbed on Au(111)

H. Yamane and N. Kosugi

Department of Photo-Molecular Science, Institute for Molecular Science, Okazaki 444-8585, Japan

Study of organic/metal interfaces is essential to investigate electronic phenomena derived from the complex interplay between van der Waals interaction and exchange-correlation interaction. Previous studies on organic/metal energetics have been performed mainly for non-ordered or multi-domain systems due to experimental difficulties. In this work, we applied the precise angle-resolved photoemission spectroscopy (ARPES) to the single-domain monolayer of coronene weakly physisorbed on Au(111).

The present experiments were performed at BL6U. The cleanliness of the Au(111) surface was confirmed by the low-energy electron diffraction with a micro channel plate (MCP-LEED) and the Shockley surface state in ARPES, as obtained from the repeated cycles of the Ar^+ sputtering ($I \sim 2 \mu\text{A}$) and the subsequent annealing ($T = 700 \text{ K}$). The total energy resolution in the present ARPES measurement was 16 meV.

Figure 1 shows (a) the LEED image and (b) the surface Brillouin zone (SBZ) of the coronene mono-layer on Au(111). The observed LEED spots show the (4×4) single-domain superstructure with respect to the Au(111) hexagonal surface lattice.

The energy-*vs*-momentum $E(\mathbf{k})$ contour maps of the clean Au(111) surface and the coronene/Au(111) superstructure, obtained from ARPES, are shown in Fig. 2(a) and 2(b), respectively. Upon the formation of the coronene/Au(111) superstructure, some new electronic states are observed. The free-electron-like dispersive bands are weakly appeared near the Fermi level E_F ($E_b = 0 \sim 0.4 \text{ eV}$) and the Au 5d band ($E_b = 1.7 \sim 2.4 \text{ eV}$). The inflection point of these parabolic dispersions appears at the $\bar{\Gamma}$ point of the monolayer's SBZ ($k_{\Gamma\text{K}} = 1.08 \text{ \AA}^{-1}$). The parabolic dispersions at the low and high E_b side may originate from the Shockley- and Tamm-type interface states, respectively, both of which are induced by the surface potential due to the presence of the coronene superstructure. Here, the E_b position of the parabolic dispersions are almost the same for the original Shockley and Tamm surface states of the clean Au(111) surface. Therefore, the interface interaction between coronene and Au(111) is considered to be quite weak.

At $E_b \sim 1.6 \text{ eV}$, a highest occupied molecular orbital (HOMO) peak is observed. The energy distribution curve at $k_{\Gamma\text{K}} = 1.40 \text{ \AA}^{-1}$ shows a sharp HOMO line shape with the high- E_b satellite due to the hole-vibration coupling. This observation also suggests the weak physisorption between coronene and Au(111). Note that, the HOMO peak shows a quite weak but non-negligible dispersion of $\sim 20 \text{ meV}$. The in-plane band dispersion of molecular electronic states has been observed for strongly chemisorbed interfaces with larger dispersion of $0.2 \sim 0.3 \text{ eV}$ due to the interfacial orbital hybridization [1,2]. Judging from the present experimental evidence, the observed in-plane band dispersion is ascribed to the genuine intermolecular interaction in two-dimensional sheets of aromatic hydrocarbons.

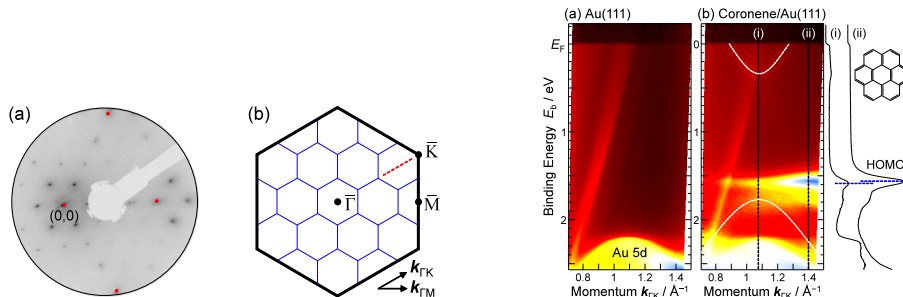


Fig. 1. (a) The MCP-LEED image of the coronene monolayer on Au(111) at 15 K, taken with the 70-eV incident electron beam. The red spot indicates the substrate's spot. (b) The surface Brillouin zone (SBZ) of the monolayer superstructure of coronene on Au(111). The black and blue solid lines indicate the substrate and monolayer SBZs, respectively. The red dashed line indicates the scan region of ARPES.

Fig. 2. The $E(\mathbf{k})$ map at $T = 15 \text{ K}$ around the 2nd $\bar{\Gamma}$ point in the monolayer's SBZ [cf. Fig. 1(b)]; (a) The clean Au(111) surface. (b) The coronene monolayer on Au(111) with the energy distribution curve at (i) $k_{\Gamma\text{K}} = 1.08 \text{ \AA}^{-1}$ and (ii) $k_{\Gamma\text{K}} = 1.40 \text{ \AA}^{-1}$. The molecular structure of coronene is also shown.

[1] H. Yamane *et al.*, Phys. Rev. B **76** (2007) 165436.

[2] M. Wießner *et al.*, Nat. Commun. **4** (2013) 1514.

Linearly-Dispersive Electronic States at the Interface of Organic Monolayers on Graphite

H. Yamane and N. Kosugi

Department of Photo-Molecular Science, Institute for Molecular Science, Okazaki 444-8585, Japan

Organic monolayers on solid surfaces show various electronic states and complex electronic phenomena, depending on electronic interactions at their interface. Some interfacial electronic phenomena, such as the charge transfer, have been applied to the control of interface energetics in functional molecular systems. In this work, by using angle-resolved photoemission spectroscopy (ARPES), we succeeded in observation of a linearly-dispersive electronic state at the interface of organic monolayers on graphite.

The present work was performed at BL6U. The single-crystalline graphite (Gr) was obtained by the direct resistive heating of a 6H-SiC(0001) wafer at 1500°C [1], as confirmed by the low-energy electron diffraction (LEED) and the valence band dispersion. In order to obtain the well-ordered organic monolayer, the Gr substrate was heated at 100~120°C during the deposition at 1~2 Å/min. The energy resolution in the present ARPES experiment was 16 meV at 15 K.

Figure 1(a) shows the LEED image of the metal-free phthalocyanine (H_2Pc) monolayer on Gr at 15 K. The observed LEED image indicates the well-known multi-domain structure for Pc molecules on six-fold symmetric surfaces. The molecular unit cell of H_2Pc on Gr determined from LEED [Fig. 1(b)] corresponds to the previous STM study [2]. Considering the symmetry of the molecular unit cell, we measured the azimuthal-angle-dependent ARPES.

Figure 1(c) shows the energy-vs-momentum $E(\mathbf{k})$ map and its energy- and momentum-distribution curves (EDC and MDC) at $h\nu = 45$ eV, for the mono-layer of H_2Pc on Gr at 15 K along the \mathbf{b}_1^* direction. The highest occupied molecular orbital (HOMO) peak appears at the binding energy (E_b) of 1.4 eV. In addition, the linearly-dispersive feature appears weakly but undoubtedly at $E_b = 0\sim2.2$ eV, like Dirac cone, as indicated by the dashed line in the $E(\mathbf{k})$ map and MDC. This is the interface-specific state, which is observable for neither the clean Gr substrate nor the thick multilayer film. In general, the Dirac cone in a honeycomb structure, such as graphene, is appeared not at the edge but at the corner of the Brillouin zone. In the present case, we found that the linearly-dispersive interface state appears at all azimuth direction. Therefore, the observed linearly-dispersive interface state could be due to the Umklapp scattering from the Dirac band of the underlying Gr substrate.

In order to elucidate the origin of the linearly-dispersive interface state in more detail, we measured ARPES as functions of temperature, substrate, and molecule. We found that the linearly-dispersive interface state is getting weak at the higher temperature (e.g., 300 K), and is not observable at the $\text{H}_2\text{Pc}/\text{Au}(111)$ interface. These results suggest the importance of the interfacial electronic coupling between organic monolayers and the Gr substrate. Furthermore, the linearly-dispersive interface state is observed also for other monolayers of pentacene, coronene, and C_{60} on Gr with different dispersion parameters such as the Fermi momentum (\mathbf{k}_F) and the Fermi velocity (v_F). On the other hand, both \mathbf{k}_F and v_F at the CoPc/Gr interface are almost the same as those at the $\text{H}_2\text{Pc}/\text{Gr}$ interface, suggesting the importance of the molecular unit cell.

Judging from the present observations, the linearly-dispersive interface state is governed by both the size of the molecular unit cell and the molecule-Gr electronic coupling. The Dirac band of the Gr substrate could be scattered and modified by the intermolecular phonons of adsorbates as a result of the surface Umklapp process, which plays a crucial role in the charge/spin extraction in molecule-graphene hybrid systems.

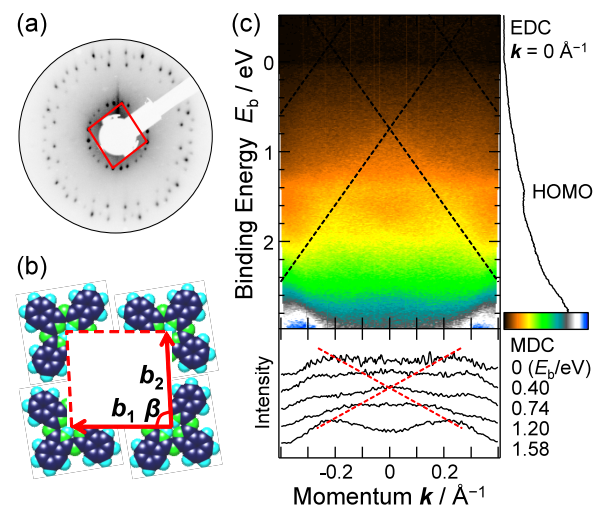


Fig. 1. (a) The LEED image of the H_2Pc monolayer on Gr at 15 K, taken with 20-eV incident electron beam. (b) The molecular unit cell of H_2Pc on Gr, where $b_1 = 13.8$ Å, $b_2 = 13.1$ Å, and $\beta = 87.6^\circ$ [2]. (c) The $E(\mathbf{k})$ map along the \mathbf{b}_1^* direction with the energy- and momentum-distribution curves (EDC and MDC) of H_2Pc on Gr at 15 K ($h\nu = 45$ eV).

[2] I. Forbeaux *et al.*, Phys. Rev. B **58** (1998) 16396, and references therein.

[3] K. Nilson *et al.*, J. Chem. Phys. **127** (2007) 114702.

Electronic structure of epitaxial, metallic germanium nanofilms on zirconium diboride thin film substrates – Identification of a new form of crystalline germanium

R. Friedlein¹, H. Yamane², N. Kosugi², Y. Yamada-Takamura¹

¹School of Materials Science, Japan Advanced Institute of Science and Technology, Nomi, Ishikawa 923-1292, Japan

²Dept. of Photo-Molecular Science, Institute for Molecular Science, Okazaki 444-8585, Japan

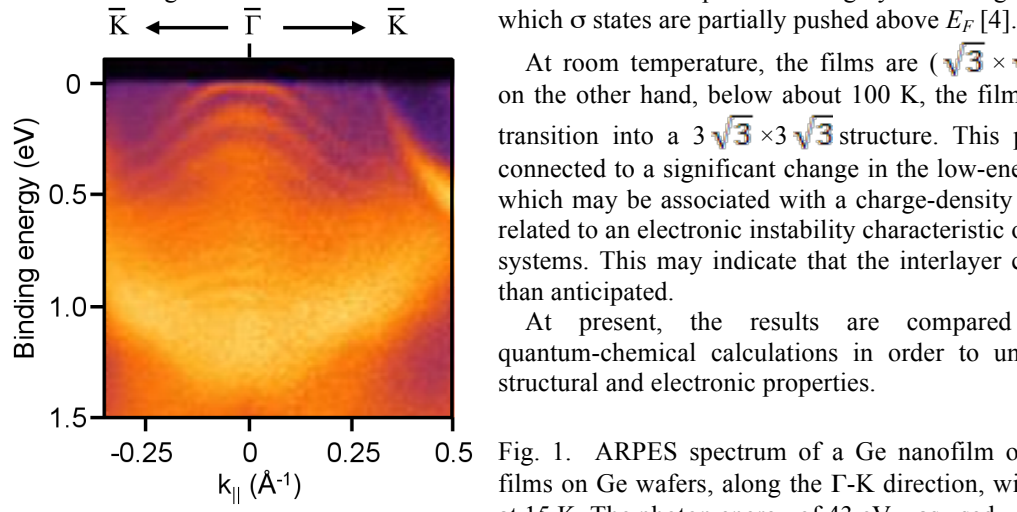
While Si and Ge are right below C in the periodic table of elements, valence orbitals for Si and Ge do not sp^2 hybridize as easily as for their smaller counterpart. However, considering the experimental evidence for the existence of the largely sp^2 -hybridized form of silicon called “epitaxial silicene” mounting [1-3], the verification of layered, hexagonal germanium structures with Dirac-cone like electronic signatures – in analogy to graphene and silicene conveniently coined “germanene” - would represent another important step towards novel two-dimensional nano-materials.

In this context, recently, in our home laboratory, we have succeeded in preparation of nanofilms of germanium on the surface of $ZrB_2(0001)$ thin films grown on Ge(111) wafers. These epitaxial, single-crystalline-like Ge nanofilms are formed by surface segregation at elevated temperatures and oxidize upon exposure to air.

However, the native oxide can be removed by an annealing procedure under ultra-high vacuum conditions upon which again Ge nanofilms are formed. At BL6U, these films have then been studied *in situ* by angle-resolved valence band (ARPES) and core-level (XPS) photoelectron spectroscopy as well as by low-energy electron diffraction (LEED).

The measured electronic and structural properties of the films are consistent with a layered structure of hexagonal symmetry and a (1×1) in-plane lattice constant that is about 20 % smaller than that of bulk germanium in the diamond crystal structure.

Figure 1 shows the valence band structure along the Γ -K direction of the (1×1) diboride Brillouin zone, as obtained at 15 K . A manifold of well-defined states with upwards curvature are observed. These states are likely thin film slab states that are related to the layered structure of the nanofilms. Some of these states cross the Fermi level indicating that the films are metallic. This behavior is expected for highly-strained germanium layers in



At room temperature, the films are $(\sqrt{3} \times \sqrt{3})$ -reconstructed; on the other hand, below about 100 K, the films undergo a phase transition into a $3\sqrt{3} \times 3\sqrt{3}$ structure. This phase transition is connected to a significant change in the low-energy band structure which may be associated with a charge-density wave ground state related to an electronic instability characteristic of low-dimensional systems. This may indicate that the interlayer coupling is weaker than anticipated.

At present, the results are compared with those of quantum-chemical calculations in order to understand both the structural and electronic properties.

Fig. 1. ARPES spectrum of a Ge nanofilm on $ZrB_2(0001)$ thin films on Ge wafers, along the Γ -K direction, with the sample held at 15 K. The photon energy of 43 eV was used.

[1] P. Vogt, P. De Padova, C. Quaresima, J. Avila, E. Frantzeskakis, M. C. Asensio, A. Resta, B. Ealet, G. Le Lay, Phys. Rev. Lett. **2012**, 108, 155501.

[2] A. Fleurence, R. Friedlein, T. Ozaki, H. Kawai, Y. Wang, Y. Yamada-Takamura, Phys. Rev. Lett. **2012**, 108, 245501.

[3] R. Friedlein, A. Fleurence, J. T. Sadowski, Y. Yamada-Takamura, Appl. Phys. Lett. **2013**, 102, 221603.

[4] Y. Wang, Y. Ding, Solid State Commun. **2013**, 155, 6.

Hydrogen Interaction on MoS₂ Surface

S. W. Han^{1,2}, Hiroyuki Yamane³, Nobuhiro Kosugi³, and Han Woong Yeom^{1,2}

¹Center for Artificial Low Dimensional Electronic Systems, Institute for Basic Science, Pohang 790-784, Korea

²Department of Physics, Pohang University of Science and Technology, Pohang 790-784, Korea

³Institute for Molecular Science, Myodaiji, Okazaki 444-8585, Japan

Recently, it has been reported that the hydrogenated MoS₂ induced a weak ferromagnetism persisting up to room temperature (RT) with the improved transport property [1]. It is important to understand the interaction between the H₂ molecule and the MoS₂ surface.

Angle-resolved photoemission (ARPES) experiments were performed at the 6U beamline of UVOSR-III in the Institute of Molecular Science. Natural and single crystalline MoS₂ samples were cleaved in the UHV. The orientation of samples was confirmed by a hexagonal pattern in low-energy electron diffraction and the band structure from the ARPES data, which were collected at 140 K in the main chamber with a base pressure of 1×10^{-10} torr. The energy and angular resolutions of the ARPES apparatus were better than 25 meV and 0.1°. The MoS₂ surface was exposed to hydrogen gas at RT by back filling the chamber with a pressure of 1×10^{-6} torr and postannealed in the preparation chamber.

Figure 1(a) shows the ARPES data of a cleaved MoS₂ surface along the Γ -K high-symmetry line of the hexagonal Brillouin zone. ARPES data were recorded with a photon energy of 100 eV and scaled by the maximum intensity. A valence band maximum (VBM) is located at the Γ -point with a binding energy of 0.34 eV. Below the VBM at Γ , there exists a strong band dispersing down (red rectangle) from the binding energy of 0.60 eV. This state is known to be a surface state, with the main contribution from the S 3p_z orbital on the top sulfur layer above the Mo layer within a topmost layer of bulk MoS₂, while the VBM originates mainly from the Mo 4d_{z²} orbital [2]. On the other hand, the top of the valence band dispersion at the K point (1.325 \AA^{-1} , vertical dashed lines), stems from the mixed states of Mo 4d_{xy/x²-y²} and S 3p_{xy} orbitals and is located at a higher binding energy of 0.80 eV than that of VBM. This confirms the indirect bandgap of bulk MoS₂.

Figure 1(b) exhibits the band structure of MoS₂ surface after an exposure to hydrogen gas for 600 s, corresponding to 600 L (1 L = 10^{-6} Torr·s). Despite of the hydrogen exposure, band structure remains unchanged. Instead, the VBM slightly shifted toward Fermi energy (E_F) and it is located at 0.26 eV with a quite obvious band dispersion. The VBM further shifts to 0.20 eV in the case of a longer exposure of a new MoS₂ surface to hydrogen gas for 3600 s (3600 L) as shown in Fig. 1(c).

In contrast, after postannealing at 300 °C for 1 h [Fig. 1(d)], the VBM is located at the binding energy of 0.75 eV, which reversely shifted away from E_F .

In order to elucidate the hydrogenation, another MoS₂ sample was cleaved and annealed at 300 °C and then exposed to hydrogen gas for 1.5 h (5400 L). In Fig. 1(e), the VBM is obtained at a much higher binding energy of 1.24 eV with slightly broadened spectral features. Especially S p_z derived bands are enhanced at the higher binding energy side.

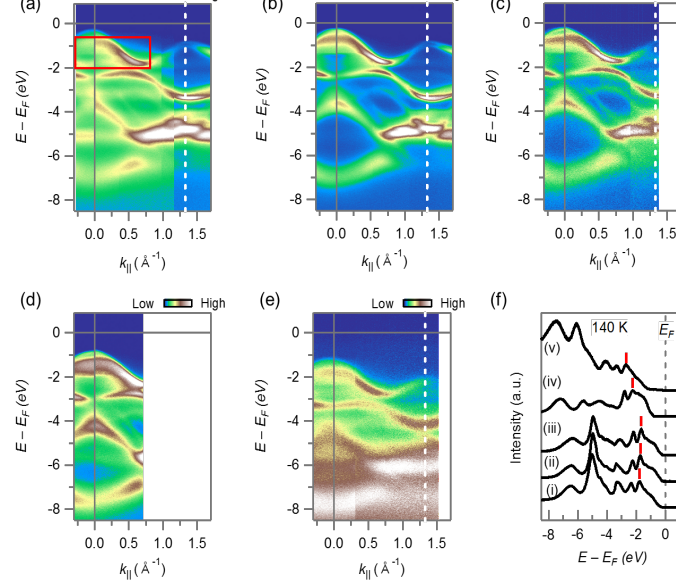


Fig. 1. ARPES intensity maps along the Γ -K direction of the Brillouin zone for three MoS₂ samples.

[1] S. W. Han *et al.*, Phys. Rev. Lett. **110** (2013) 247201.

[2] S. W. Han *et al.*, Phys. Rev. B. **86** (2012) 115105.

Figure 1(f) represents the shift of valence-band spectra, which were integrated from the ARPES data and normalized by the intensity of the first peak indicated by the (red) lines. Without a significant change of band structure, the hydrogen exposure leads to shift the VBM toward E_F while the annealing shifts the VBM away from E_F .

These results suggest that the thermal annealing promotes the dissociation of H₂

molecules on the MoS₂ surface and then the atomic hydrogens are intercalated between van der Waals gaps.